GPR143 SIGNALING ALTERS INTRACELLULAR TRAFFICKING OF PHOTORECEPTOR OUTER SEGMENTS

by

Dorothy Tung

_____

A Thesis Submitted to the W.A. Franke Honors College

In Partial Fulfillment of the Bachelor's degree

With Honors in

Neuroscience and Cognitive Science

UNIVERSITY OF ARIZONA

M A Y 2 0 2 2

Approved by:

_____

Dr. Brian S. McKay
Department of Ophthalmology and Vision Science
Department of Physiology

Abstract

Photoreceptors undergo a daily renewal process by shedding the distal 10% of their outer segments (POS), which are phagocytosed and degraded by the retinal pigment epithelium (RPE). Inefficient digestion of POS could play a role in the pathogenesis of various retinopathies and be a sign of RPE aging and reduced function. L-DOPA, a drug that appears to delay onset of age-related macular degeneration (AMD), is the ligand of a receptor in the pigmentation pathway involved in vesicular trafficking, GPR143. Here we explore whether GPR143 signaling alters the rate of POS uptake and degradation by the RPE.

We isolated POS from bovine retinas via differential ultracentrifugation and sucrose gradient sedimentation. For the uptake assay, POS were labeled with a green dye. Primary porcine RPE were challenged with POS in low tyrosine DMEM containing dialyzed FBS ± 1 μM L-DOPA for 2 hours. After the excess POS were removed, phase-contrast and fluorescent images were captured. For the degradation assay, POS were labelled with a pH sensitive dye that increases fluorescence intensity as pH decreases, such that the POS are only visible in the acidic lysosomal compartment. Primary porcine RPE were challenged with POS for 4 hours to allow endocytosis. We removed the excess POS, then added fresh low tyrosine DMEM with dialyzed FBS ± 1 μM L-DOPA. Phase-contrast and fluorescent images were captured every 8 hours for 28 hours. For both assays, the number and area of fluorescent POS were analyzed using ImageJ and statistical analysis was performed using Prism Graph.

Our results indicate that L-DOPA had no effect on POS uptake. Our data also showed that once the POS were in the lysosomal compartment, L-DOPA had no effect on the rate of degradation past 12 hours. However, the reduced number and area of POS in the RPE after 12

hours suggest L-DOPA had a significant effect between hours 4 and 12, which most likely relates to more efficient endosomal trafficking to the lysosomal compartment. These findings may highlight a mechanism by which L-DOPA protects from AMD.

This project is supported by the National Institutes of Health (NIH) under award number 5RO1 EY026544-05 (Brian S. McKay) and the Undergraduate Biology Research Program with funds from the Senior Vice Provost for Research.

1. Introduction

Age-related macular degeneration (AMD) is the leading cause of irreversible blindness in developed nations (1–3). Currently, more than 10% of the United States population over the age of 70 has AMD, and its prevalence will continue to increase as the population ages. Most AMD patients develop geographic atrophy, which involves deterioration of the macula and gradually impairs visual acuity. The remaining 10%-15% of AMD patients develop neovascular AMD, which involves the growth of new blood vessels that cause bleeding, swelling, and scarring of the macula (4–6). While neovascular AMD only accounts for a minority of AMD cases, it causes 85%-90% of vision loss from AMD.

A. 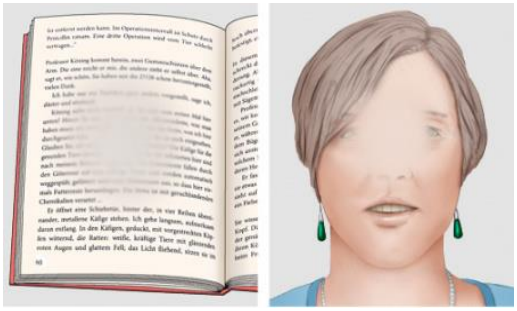 **B.** 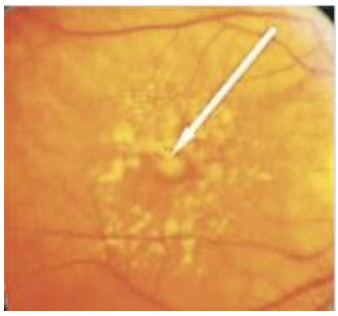

Figure 1. (A) An illustration depicting the vision of an AMD patient. Central vision is gradually lost, but peripheral vision typically stays intact. **(B)** A color fundus photograph of the posterior part of a human eye at the macula. The arrow indicates drusen deposits under the retinal pigment epithelium (RPE) in the macula associated with an intermediate level of AMD. Drusen is the accumulation of undigested proteins and lipids between the RPE and choroid (7). It leads to RPE damage and is the hallmark and diagnostic feature of AMD.

AMD incidence exhibits a striking racial bias, with Caucasians affected seven times more often than any other population after the age of 80 (8–11). We hypothesize that RPE

pigmentation, likely different among races, plays a role in this bias (12,13). Despite years of study, the etiology of AMD is unknown, and we cannot prevent the disease (14,15). However, we do know that being Caucasian is an even greater risk factor for AMD than age is past 75 years of age (Figure 2).

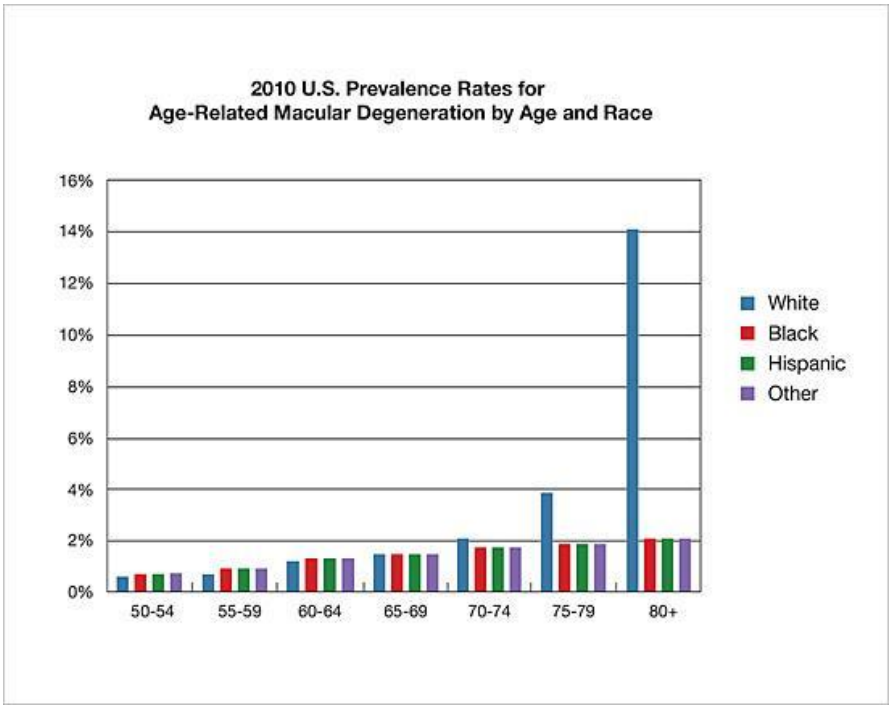

Figure 2. AMD incidence by race and age, adapted from the National Eye Institute. Graph portrays the percentage of the population by age and race that have AMD in 2010. Note that the rate of AMD incidence for the white population rises exponentially after 75 years of age. In contrast, AMD incidence in all other races increases more subtly as they age.

To understand the racial bias of AMD, we investigated the melanin synthesis pathway in the retinal pigment epithelium (RPE), a monolayer of cells located between the neural retina and choroid (Figure 4). The pigmentation pathway includes GPR143, a little studied G-protein coupled receptor (GPCR) at the apical surface of the RPE. We discovered that its ligand was L-

DOPA, which is a byproduct of melanin synthesis, through oxidation of tyrosine by the enzyme tyrosinase (16).

Figure 3. Phase contrast image of primary porcine RPE taken using the 5X objective. RPE is characterized by five main epithelial features: polygonal shape, apical/basal polarity, pigmentation, and they are post-mitotic, phagocytic cells (17).

GPR143 expression is limited to melanin-containing cells (18). The expression of GPR143 in cells that also produce melanin and L-DOPA indicates that GPR143 signals in an autocrine manner (16). Mutations in the gene encoding GPR143 cause ocular albinism (OA), a condition where pigmented cells accumulate melanin, but in mishappen macromelanosomes (18,19). This observation indicates GPR143 signaling has a function in endosomal trafficking, because melanin formation is normal, but vesicular accumulation is flawed (19–21). The lack of effects on cutaneous or ocular pigmentation underscores the point that GPR143 signaling does not control melanin production. However, OA carries all the visual hallmarks of albinism: misrouting of the optic nerve projection at the optic chiasm, foveal hypoplasia, and decreased numbers of photoreceptors and ganglion cells—together, resulting in poor vision (22). Thus, the visual defects in albinism occur from either loss of the ligand, L-DOPA, which is produced as a byproduct of melanin, or loss of the receptor, GPR143.

GPR143 activation by L-DOPA increases expression of pigment epithelium-derived factor (PEDF), the most potent neurotrophic factor in the eye (16). Conversely, GPR143 signaling decreases RPE secretion of vascular endothelial growth factor (VEGF), a potent angiogenic factor (21). Reducing ocular VEGF likely fosters a reduced angiogenic environment in the RPE. Further illustrating this important finding, the current treatments for neovascular AMD are anti-VEGF therapies, however, this requires costly monthly intravitreal injections that are unpleasant and expensive (4).

To explore whether GPR143 signaling affects AMD, a retrospective analysis of electronic medical records from over 87 million people was conducted to compare the AMD incidence and age of onset between patients taking and not taking L-DOPA (23). We found that AMD onset was both reduced and delayed in patients prescribed L-DOPA, primarily for movement disorders such as Parkinson's Disease. L-DOPA delayed the age of onset of AMD from 71.4 years to 79.3 years in patients with geographic atrophy, and from 75.5 years to 80.8 years in patients with neovascular AMD.

In a proof of principle prospective clinical trial, L-DOPA significantly improved visual outcomes and was well-tolerated under treatment for neovascular AMD. L-DOPA increased the best corrected visual acuity, decreased subretinal fluid accumulation, and decreased the mean central retinal thickness in patients with neovascular AMD (24). Thus, L-DOPA positively affected the cardinal symptoms of neovascular AMD. Furthermore, patients taking L-DOPA required significantly fewer anti-VEGF injections to decrease angiogenesis. These findings indicate that L-DOPA is efficacious in treating neovascular AMD and could serve as an adjuvant to anti-VEGF injection therapy. This, in turn, would reduce the pain and financial burden associated with treatment of the disease. According to the Centers for Medicare and Medicaid

Services, anti-VEGF therapy for neovascular AMD represents the second leading healthcare expenditure in the United States: over 8.2 billion dollars per year.

While L-DOPA appears to be a promising treatment for AMD, its underlying mechanisms remain unclear. Thus, we seek to investigate one potential mechanism by which GPR143 signaling may function to delay or halt AMD progression: the photoreceptor outer segment (POS) digestion process. In my project, I explore whether GPR143 signaling affects the POS uptake and degradation process to unveil a potential mechanism by which L-DOPA protects against AMD.

2. Background

2.1 Ocular Anatomy

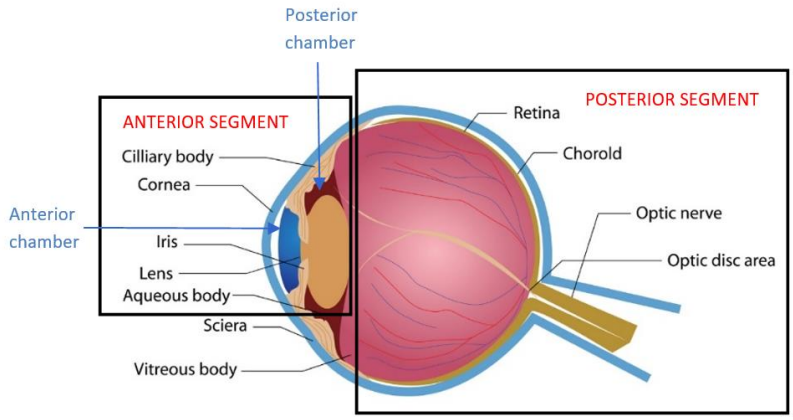

Figure 4. Ocular anatomy, adapted from the Armenian EyeCare Project. A sagittal view of an eye illustration with key features labeled.

The eye can be discussed as two segments: the anterior and posterior. The anterior segment of the eye includes the aqueous humor, cornea, iris, pupil, lens, and ciliary body (25). The anterior segment is further separated into two chambers: the anterior and posterior. The

anterior chamber is filled with aqueous humor, a clear fluid between the cornea and lens that supplies nutrients to regions lacking blood vessels (26). The cornea is the clear, protective outer layer of the eye that serves as a barrier to the external environment and is also responsible for most of the light refraction. The colored part of the eye is the iris; it divides the anterior chamber from the posterior chamber. The pupil lies at the center of the iris and adjusts its size with the iris dilator and sphincter muscles based on the levels of light. The lens lies in the posterior chamber and fine tunes the focus of light onto the retina. The ciliary body produces aqueous humor which nourishes the avascular anterior chamber and contains ciliary muscles at the base that control the shape of the lens to focus on objects at different distances (27). With aging, the lens gradually loses its ability to focus well, leading to a common condition called presbyopia where it is difficult to see nearby objects clearly (28).

The posterior portion of the eye includes the vitreous humor, retina, choroid, and optic nerve (26). The vitreous humor is a clear, jelly-like substance that fills the posterior segment of the eye. The retina consists of two distinct parts: the neural sensory retina and the RPE. The neural sensory retina contains photoreceptors (rods and cones) that signal in response to light. Rods function best in dim light settings like at night and do not perceive color, only how bright the environment is. There are three types of cones that respond to either blue, green, or red light. A region of the retina known as the macula contains a high concentration of cones and contributes to sharp visual acuity and color vision. The RPE is located between the photoreceptors and the choroid, which is the vascular supply of the outer retina and photoreceptors. The RPE performs a variety of functions that support the retina including transporting nutrients, recycling retinal visual pigments, digesting shed outer segments, and absorbing scattered light (29). The choroid is abundant in leaky, fenestrated blood vessels and

nourishes the RPE, which transport the nutrients to the photoreceptors. Finally, the optic nerve extends from the retina, leaving the eye at the optic disc, and then connecting to the brain. Since the optic disc does not contain any photoreceptors, it corresponds to the blind spot in our visual field.

2.2 Photoreceptor Renewal

Photoreceptors undergo a daily renewal process by shedding the distal 10% of their outer segments while continuously generating new discs that make up the outer segment at the proximal end (30). While disc shedding occurs intermittently once per day, new disc assembly occurs continuously. After the inner segment synthesizes proteins for the outer segment, the proteins are transported toward the connecting cilium for insertion into the outer segment. This allows photoreceptors to maintain a constant length despite daily shedding (Figure 5), while also rejuvenating the visual system throughout our lives.

There are several differences between the renewal of rods and cones (31). Previous studies suggest that rod outer segment turnover is significantly faster than that of cone outer segments, with rods fully shedding 10% once a day while only one-fifth of cones shedding daily in goldfish (32). Moreover, rods typically shed at light onset, while cones shed at nighttime. Rhodopsin is the light-sensitive protein found in rods, while iodopsin is the light-sensitive protein found in cones.

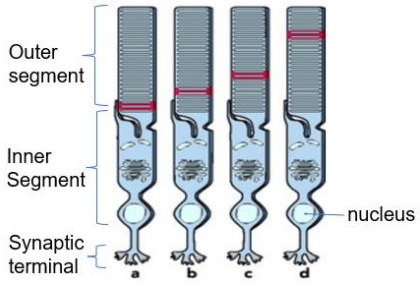

Figure 5. Photoreceptor renewal, adapted from Kevany and Palczewski (2010) and representing the findings of Bok and Young. The red radioactive band represents the same disk moving down the photoreceptor over time with successive daily renewals.

The RPE plays a critical role in photoreceptor renewal with the daily engulfment and degradation of the shed POS. Often overlooked, this daily activity makes the RPE the most phagocytic tissue in the body (17,33–35). Each RPE cell phagocytoses POS from approximately 30 photoreceptors, and it is estimated that each human RPE cell has digested 10^8 shed outer segments by 80 years of age. This digestive process involves a series of temporal steps: recognition, binding, intracellular signaling, internalization, and digestion (34). During POS recognition and binding, milk fat globule-EGF-factor 8 (MFG-E8) serves as a bridge protein, binding to the integrin receptor αvβ5 on the RPE surface and the phosphatidylserine (PS) on the POS surface (36). CD36 is another receptor at the RPE surface that binds to PS and plays a role in POS binding (37). To signal POS engulfment, MertK—a receptor tyrosine kinase at the surface of the RPE—binds to Gas 6 and Protein S through other bridge protein ligands (38). POS engulfment requires a series of signaling events, followed by cytoskeleton reorganization for pseudopod extension. Once internalized, the phagosome fuses with early endosomes, late endosomes, and eventually the lysosome (Figure 6). In the lysosome, POS are degraded by proteases—primarily by cathepsin D in RPE (39). Inefficient digestion of POS leads to the aggregation of lipids and proteins within the RPE, likely playing a role in the pathogenesis of various retinopathies including AMD.

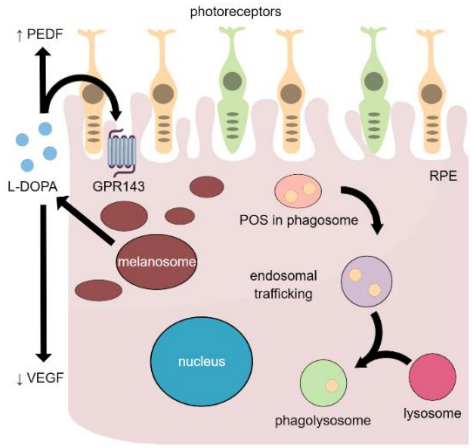

Figure 6. An overview of two critical pathways in the RPE: GPR143 signaling and POS degradation.

3. Methods

3.1 RPE Cultures:

Primary RPE cultures were prepared from freshly enucleated porcine eyes. The anterior segment, vitreous body, and retina were removed to expose the apical surface of RPE for culture. 500 µL of Versene, an EDTA solution used as a calcium chelator and non-enzymatic cell dissociation reagent, was added to each eyecup. After a gentle rinse, the Versene was removed. 1 mL of 0.25% Trypsin, a protease dissolved in Versene to digest cell junctions, was then added to each eyecup and incubated for 30 minutes to detach the RPE cells from the Bruch's membrane. Following the incubation, the cell suspension was transferred to a conical tube and an equal volume of Dulbecco's modified essential medium (DMEM) with fetal bovine serum (FBS) to trypsin was mixed in. The FBS inactivates the trypsin so that the RPE cell membranes are not damaged. A small volume of this suspension was transferred back to the eyecups and was gently pipetted up and down to collect the remaining RPE cells. The conical tube containing the cell

suspension was centrifuged at 500xg for 5 minutes. The supernatant was removed, and the pellet of cells was resuspended in DMEM with FBS and antibiotic-antimycotic. This cell suspension was gently pipetted up and down to break up any cell clumps before transfer to a 25 cm^2 flask. The primary RPE cells were passaged once or twice before the start of an experiment.

3.2 POS Isolation:

POS were isolated from freshly enucleated bovine eyes using previously published methods (40). The anterior segment and vitreous body were removed to expose the retina, which was then detached using a pair of forceps. 12 bovine retinas were suspended in 30% sucrose in 5 mM HEPES on ice. The retinas were pelleted by centrifugation at 27,800xg for 30 minutes at 4°C. Isolated retinas were homogenized by 30 brisk strokes using a Dounce homogenizer, creating a retinal homogenate. The retina homogenate was loaded onto a discontinuous sucrose gradient (26%, 32%, 36%) and centrifuged at 49,400xg for 30 minutes at 4°C. Using a glass pipette, samples of the top and bottom diaphanous POS layers were loaded onto separate microscope slides. These slides were viewed under a microscope to determine which layer of POS from the sucrose gradient had the most intact outer segments. The layer with debris was retrieved and centrifuged at 1000xg for 5 minutes at 4°C to remove any debris. The pellet was disposed of, and the supernatant containing the purified POS was resuspended in 5mM HEPES. The POS were then washed again in HEPES, and pelleted at 27,800xg for 30 minutes at 4°C. The subsequent pellet was resuspended in sterile-filtered 5% sucrose in 5mM HEPES, then stored at -20°C.

3.3 Western Blot:

A Western Blot analysis was performed to characterize the purified POS (Figure 8). Two POS samples of different volumes were sonicated for 5 seconds before they were loaded onto separate

lanes of the 12% polyacrylamide gel for separation by SDS-PAGE. Lonza RPE cell lysate was also loaded onto the gel to serve as a negative control. Since rhodopsin is the most prevalent protein found in POS, we probed with an anti-rhodopsin antibody (1:5000) to verify our particles were POS. We also probed with anti-cytochrome c oxidase IV (COX IV 1:1000) and anti-melanocyte inducing transcription factor (MITF 1:1000) antibodies. COX IV is an enzyme complex localized to the inner mitochondrial membrane that is involved in oxidative phosphorylation and serves as a mitochondrial marker. MITF is a transcription factor that plays a role in melanogenesis as well as the regulation of RPE development and differentiation. It is shuttled between the nucleus and cytoplasm, and can serve as a nuclear marker for RPE while doubling as a negative control for POS (41). In a purified POS sample without mitochondria or RPE nuclei, we would only expect to detect rhodopsin. In the Lonza RPE cell lysate, we would expect to detect COX IV and MITF, but not rhodopsin.

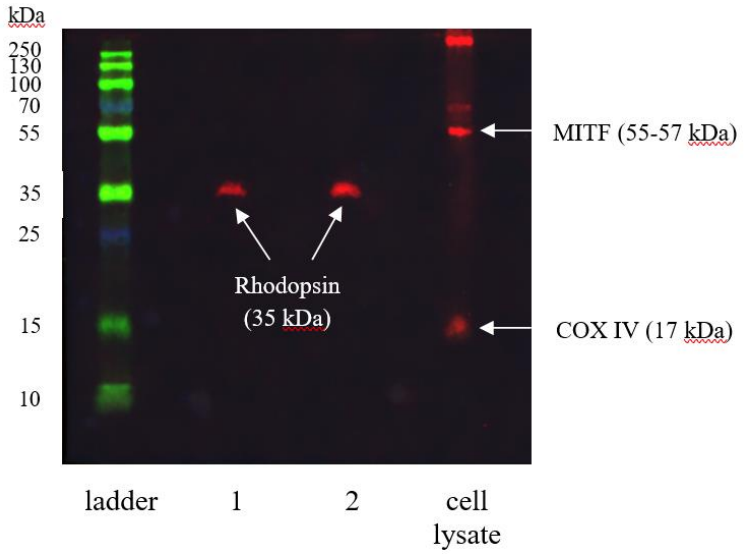

Figure 8. Western blot illustrating rhodopsin at 35 kDa in purified bovine POS. The first lane on the left is the PageRuler protein ladder. No COX IV or MITF bands appeared in the two middle lanes loaded with purified POS, only a rhodopsin band. The final lane on the right was loaded

with 20 μg protein of Lonza RPE cell lysate. No rhodopsin band appeared, however, there were visible bands for COX IV at 17 kDa and MITF at 55-57 kDa. This demonstrates the purity of the POS isolation.

3.4 Labeling POS with Vybrant DiO Cell-Labeling Solution:

To track POS uptake by the RPE, the POS were labeled with Vybrant DiO Cell-Labeling Solution, a green fluorescent dye. The POS were first suspended in serum-free culture medium at a concentration of $1x10^6$/mL. 5 μL of the dye was added per mL of the POS suspension. The suspension was mixed well by gently pipetting before incubating for 20 minutes at 37°C. Following the incubation, the labeled suspension was centrifuged at 1250xg for 30 minutes at 4°C. The supernatant was removed and the labeled pellet was resuspended in warm medium. This final wash step was repeated two more times.

3.5 POS Uptake Assay:

Porcine RPE were plated on an 8-well chambered coverglass slides and grown to confluency before starting the assay. After the POS were labeled with Vybrant DiO Cell-Labeling Solution, they were counted using a hemocytometer and loaded into each well along with 250 μL of low tyrosine (LT) DMEM with dialyzed fetal bovine serum (dFBS) and antibiotic-antimycotic. The medium must contain low levels of tyrosine, because a previous study suggests that cell surface expression of GPR143 is tyrosine-sensitive (16). Standard culture medium with 500 μM tyrosine results in GPR143 internalization without activation, making tyrosine a receptor antagonist. However, GPR143 was detected on the plasma membrane of RPE cells in tyrosine-free medium and medium with low concentrations of tyrosine (1 μM). Dialyzed FBS must also be used, because the concentrations of small molecules like amino acids, especially tyrosine, are

significantly reduced during dialysis. RPE cells were incubated with POS in the presence or absence of 1 μM L-DOPA for 2 hours. After 2 hours, the nonphagocytosed, excess POS, were removed, the cells were gently rinsed, and 250 μL of fresh LT DMEM with dFBS was added into each well. Using the 40X objective at an exposure of 45.4 ms, 4 phase contrast and 4 fluorescent images were taken in each well. The number and total area of fluorescent POS in each image were quantified using ImageJ. ImageJ software was setup to automatically identify, count, and measure the size of the POS in each image.

3.6 Labeling POS with pHrodo Green (Thermo Fisher):

To track POS degradation in the lysosome, the POS were labeled with pHrodo Green (Thermo Fisher), a pH sensitive dye that increases fluorescence intensity as pH decreases, such that POS only fluoresce in the acidic lysosomal compartment. A 0.1 M sodium bicarbonate buffer with pH 8 ± 0.05 was freshly prepared and sterile-filtered. 50 μL of DMSO was added per 100 μg of dye. The sodium bicarbonate buffer was added to the dye at 10 times the volume of the DMSO. The POS were incubated in this solution for 30 to 60 minutes in the dark. After the incubation, the solution was centrifuged at 5000xg for 10 minutes at 4°C. The supernatant was removed and the labeled POS were resuspended in sterile 5% sucrose in 5 mM HEPES.

3.7 POS Degradation Assay:

Porcine RPE were plated on 8-well chambered coverglass slides and grown to confluency prior to starting the assay. Using the 40X objective at an exposure of 159.6 ms, 5 phase contrast and 5 corresponding fluorescent images were taken of the wells before POS were introduced to account for cellular autofluorescence. This photography protocol was used for all experiments to maintain consistency. This represents time 0 of the degradation assay. After the POS were

labeled with pHrodo Green (Thermo Fisher), they were counted using a hemocytometer and 2 POS per cell were loaded into each well along with 250 μL of LT DMEM with dFBS and antibiotic-antimycotic. The POS were incubated with the RPE for 4 hours to permit cellular internalization. The excess POS were removed, the cells were gently rinsed, and fresh LT DMEM with dFBS was added in the presence or absence of 1 μM L-DOPA. Additional phase contrast and fluorescent images were taken at 8-hour time points up to 28 hours. The number and total area of fluorescent POS in each image were quantified using ImageJ. Over the course of this experimental series, we analyzed over 1600 images using the same settings to produce the data we present.

4. Results

The images taken during the POS uptake assay (see Methods 3.5) were analyzed for the number of fluorescent particles and the total area of fluorescence using ImageJ. Microsoft Excel and Prism software were then used to analyze the data and test for statistical significance between the control group and L-DOPA treatment using paired t-tests (Figure 9). There is no significant difference in the number of fluorescent particles or total area of fluorescence between the control group and L-DOPA treatment at 2 hours after POS introduction, indicating uptake was not affected.

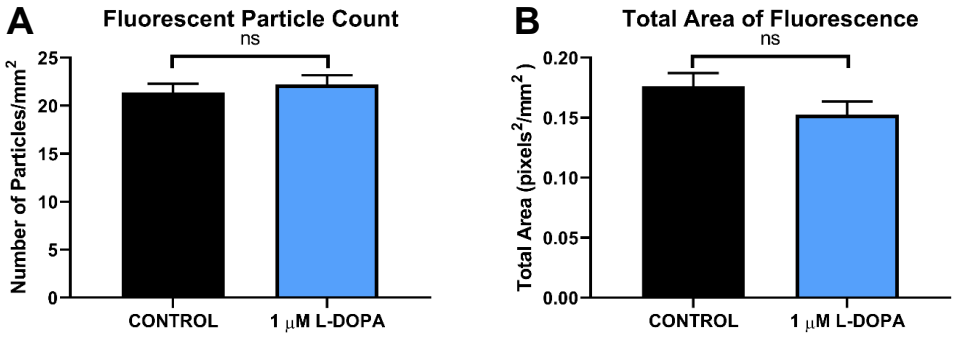

Figure 9. POS uptake by RPE at 2 hours. Displays findings from 2 separate experiments with 4 replicates each. **(A)** Quantification of the number of fluorescent particles in the control group versus L-DOPA treatment per mm^2 at 2 hours after POS introduction. **(B)** Quantification of the total area of fluorescence per mm^2 in the control group versus L-DOPA treatment at 2 hours after POS introduction.

Representative images taken during the POS degradation assay (see Methods 3.7) for the control group and L-DOPA treatment are shown below (Figure 10). 8 separate experiments were conducted with 3 to 4 replicates each.

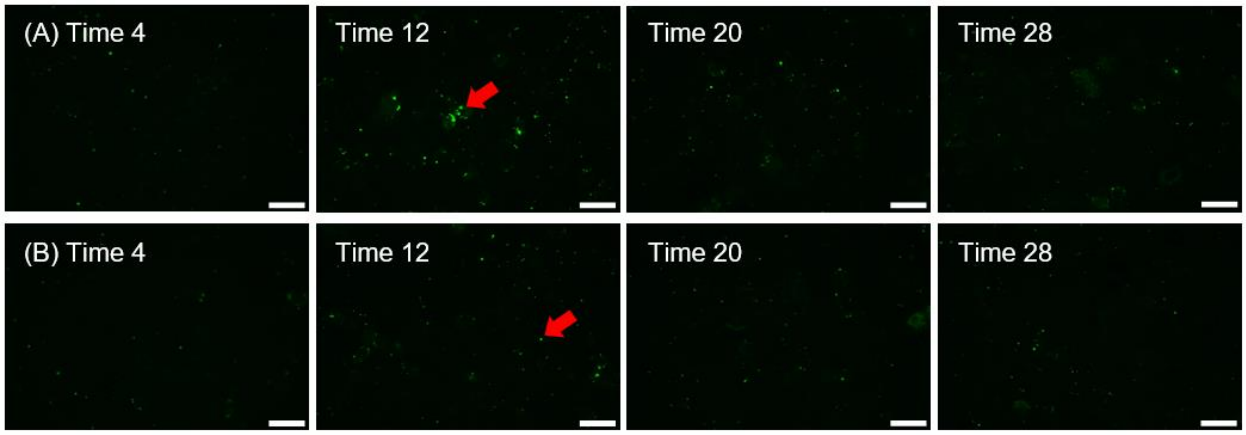

Figure 10. Porcine RPE challenged with 2 POS/cell and followed for up to 28 hours. Particle presence was evaluated using fluorescent microscopy with the 40X objective and an exposure of 159.6 ms. Red arrows indicate POS in the acidic lysosome. Scale bar = 20 μm. **(A)** Control group. Images captured at 4, 12, 20, and 28 hours after POS introduction. **(B)** L-DOPA treatment. Images captured at 4, 12, 20, and 28 hours after POS introduction.

Microsoft Excel and Prism software were used to analyze the data and test for statistical significance. Only 3 of 8 experiments achieved statistical significance between the control group and L-DOPA treatment using paired t-tests.

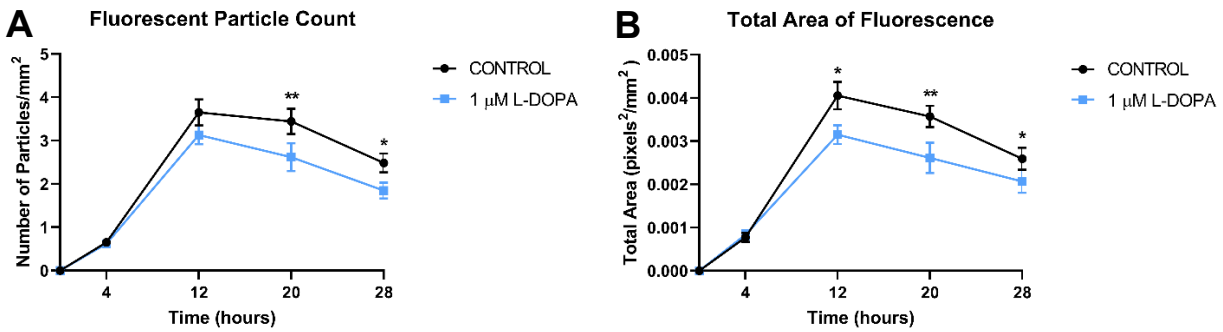

Figure 11. POS degradation by RPE over time. Representative of findings from 3 of 8 separate experiments with 4 replicates each. Results varied between experiments, perhaps due to differing levels of pigmentation and GPR143 expression in the primary RPE. There is no significant difference between the control and L-DOPA treatment at 4 hours. The L-DOPA trend is consistently lower than the control after 12 hours, however, the rate of degradation is apparently similar. **(A)** Quantification of the number of fluorescent particles per mm^2 over time. **(B)** Quantification of the total area of fluorescence per mm^2 over time. * p-value < 0.05, ** p-value < 0.005

Microsoft Excel and Prism software were used to compare the fluorescent particle count and total area of fluorescence of the L-DOPA treatment relative to the control group at each time point during the assay. Data analysis was performed using paired t-tests. At 4 hours, there is no significant difference in the fluorescent particle count or the total area of fluorescence between the control group and L-DOPA treatment. At 12 hours, there is a significant difference in the fluorescent particle count (72.0 ± 6.28% of control, $p<0.005$, n=60) and the total area of fluorescence particle area (74.9 ± 6.59% of control, $p<0.005$, n=60) in RPE treated with L-DOPA. At 20 hours, there is a significant difference in the fluorescent particle count (76.3 ± 5.91% of control, $p<0.005$, n=60) and the total area of fluorescence (79.3 ± 6.85% of control, $p<0.05$, n=60) in RPE treated with L-DOPA. This difference continued at 28 hours, as the

particle count was 70.0 ± 6.31% of control, p<0.005, n=60 and the total area of fluorescence was 70.2 ± 7.07% of control, p<0.005, n=60.

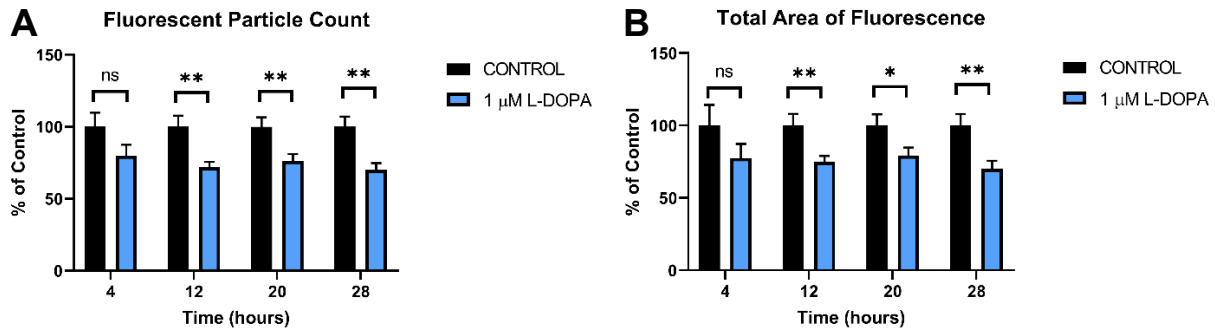

Figure 12. Comparison of POS in the RPE between control and L-DOPA treatment. Displays findings from 3 separate experiments with 4 replicates each. Results varied between experiments, perhaps due to differing levels of pigmentation and GPR143 expression in the primary RPE. GPR143 is expressed as part of the pigmentation pathway, and nonpigmented cells fail to express GPR143 as well as tyrosinase. There is no significant difference in POS uptake measured at 4 hours. However, cells treated with L-DOPA have significantly less POS remaining at 12, 20, and 28 hours. **(A)** Percent difference in the number of POS in L-DOPA treatment compared to the control group. **(B)** Percent difference in the total area of POS in L-DOPA treatment compared to the control group. * p-value < 0.05, ** p-value < 0.005

Current experiments are assessing the levels of pigmentation in primary RPE to explore whether differences in GPR143 expression contributes to the variability in results (Figure 13).

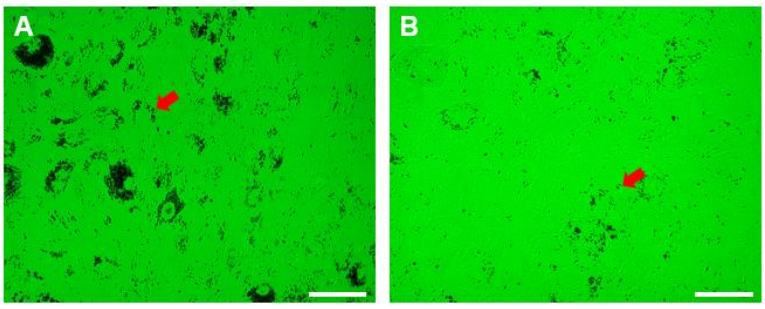

Figure 13. Phase contrast images displaying levels of pigmentation in primary RPE. Evaluated using microscopy with 40X magnification. Red arrows indicate melanin granules. Scale bar = 20 μm. **(A)** An image from an experiment that displayed statistical significance in the number and total area of POS between the control group and L-DOPA treatment. **(B)** An image from an experiment that did not display statistical significance in the number and total area of POS between the control group and L-DOPA treatment.

5. Discussion

Despite decades of research, effective treatment options for AMD are limited and many of its underlying mechanisms remain unknown. Based on data collected from a nationwide retrospective study and a proof of principle prospective clinical trial, L-DOPA appears to be a promising, financially accessible drug to treat and delay AMD. Interestingly, patients taking L-DOPA for Parkinson's disease were diagnosed with AMD less frequently and significantly later than patients not taking L-DOPA (23). Neovascular AMD patients prescribed L-DOPA also noticed improved visual outcomes and stabilized AMD-related retinal symptoms (24). To better understand how L-DOPA protects against AMD, previous studies explored how L-DOPA affects the secretion of neurotrophic factors including PEDF and VEGF. L-DOPA was found to upregulate PEDF expression and downregulate VEGF expression. The results were significant, but subtle. The robust 7-fold racial bias in AMD incidence seems unlikely to be from the subtle alterations in PEDF and VEGF. Hence, this project seeks to explore another pathway by which L-DOPA may positively affect AMD: the POS digestion process. This offers a different perspective of how L-DOPA may potentially function to ameliorate AMD in a quick and robust manner.

To explore whether GPR143 signaling affects the POS uptake process, RPE were challenged with POS ± 1 μM L-DOPA for 2 hours. Images were acquired and analyzed for the number of fluorescent particles and total area of fluorescence. The results suggest that L-DOPA had no effect on POS engulfment by the RPE at 2 hours after POS introduction. Since only 2 separate experiments were conducted using optimal POS concentrations and exposure settings, more trials should be performed to strengthen this early data for publication.

To explore whether GPR143 signaling affects the POS degradation process, RPE was challenged with labeled POS for 4 hours, after which degradation over time could be tested. After the excess POS were removed, fresh LT DMEM with dFBS ± 1 μM L-DOPA was added and images were acquired. Images were also taken at 12, 20, and 28 hours after POS introduction to be analyzed for the number of fluorescent particles and total area of fluorescence. The results suggest that L-DOPA did not alter phagocytosis and uptake, as it had no effect on the number and total area of POS in the RPE at 4 hours. L-DOPA also had no effect on the rate of degradation after 12 hours, indicating that L-DOPA does not increase the speed at which RPE digest POS. However, the reduced number and total area of POS in the RPE after 12 hours indicate that L-DOPA had a significant effect between hours 4 and 12, which most likely relates to more efficient endosomal trafficking to the lysosomal compartment. This idea aligns with GPR143's proposed role in vesicular trafficking. Previous studies suggest that GPR143 regulates membrane traffic between lysosomes and melanosomes (19). Additionally, GPR143 was found to redistribute the mannose-6-phosphate receptor (M6PR), which cycles between the trans-Golgi network and the late endosomal compartment to deliver lysosomal enzymes to the late endosome (42). Further study is needed to understand the mechanisms of how GPR143 signaling affects POS trafficking to the lysosome.

3 of 8 separate experiments displayed statistical significance between the control group and L-DOPA treatment. We believe that this variability relates to the differing levels of pigmentation in primary RPE among experiments. While all the cells used were only passaged once or twice, some exhibited much greater pigmentation than others. At the first step of the melanin synthesis pathway, tyrosinase catalyzes the conversion of tyrosine to L-DOPA. Therefore, primary RPE with greater levels of pigmentation produce more L-DOPA, serving as a confounding variable in the project. Further complicating this analysis is that both tyrosinase and GPR143 expression is driven by the same MITF-M transcription factor, such that greater pigmentation relates to greater GPR143 expression, but then also higher levels of the endogenous ligand, L-DOPA. In such case, testing for activity with exogenous L-DOPA becomes difficult, Current experiments aim to address this limitation by assessing levels of RPE pigmentation to determine whether differences in GPR143 expression may be related to variation in MITF-M, tyrosinase, and endogenous L-DOPA, causing inconsistent results.

Overall, these results illustrate another mechanism by which L-DOPA impacts AMD incidence, pathogenesis, and treatment. Impaired or delayed digestion of shed POS contributes to the pathobiology of AMD and compromises retinal health. Improved efficiency of endosomal trafficking to the lysosome compartment via GPR143 signaling leads to greater clearance and recycling of POS. This is a promising finding, however, more extensive research is needed to develop a more comprehensive understanding of the mechanism.

6. Future Direction

6.1 Basic Science Experiments:

To better understand how GPR143 signaling affects POS trafficking, future experiments will investigate whether L-DOPA alters the activity of vesicular trafficking proteins such as Rab family members. There are over 60 Rab proteins, all of which are small GTPases. Rab proteins regulate vesicle formation, membrane fusion, and actin- and tubulin-dependent vesicle transport (43). A GTPase assay could evaluate whether GPR143 signaling recruits a greater number of Rab proteins and affects the efficiency of vesicle fusion (44).

Current experiments are exploring whether L-DOPA affects the amount of lysosomal proteases made, including cathepsin D, the main protease involved in POS degradation (45). Preliminary results from a cathepsin D assay illustrate that the levels of cathepsin D are not significantly different in RPE treated with L-DOPA. Hence, future studies will utilize gel zymography to compare the total proteolytic activity between RPE in the control group versus those treated with L-DOPA. Zymography is an SDS-PAGE technique that detects proteases by analyzing their ability to degrade a protein, for example gelatin, resident as a substrate cast with the gel. At the conclusion, the gel is stained with Coomassie Blue to reveal total protein, and the proteolytically cleaved proteins are absent from the gel, leaving those regions unstained and clear.

6.2 Clinical Experiments:

A future clinical experiment could assess the levels of drusen formation in patients taking L-DOPA. Drusen is the hallmark of AMD and consists of undigested proteins and lipids that buildup between the RPE and choroid (7). They develop naturally with age and become concerning when there is an abnormal amount of large drusen. Since L-DOPA has been shown to reverse and delay the signs of AMD, this study would evaluate whether GPR143 signaling has an

inhibitory effect on drusen formation. To extend this study further, drusen deposits can also be assessed in patients with Parkinson's disease. Since Parkinson's disease patients taking L-DOPA were diagnosed with AMD significantly less often than the population at large, and at a later age compared to those not taking L-DOPA, it would be intriguing to investigate whether Parkinson's disease patients have reduced amounts of drusen compared to others of the same age.

Another experiment could explore the effect of L-DOPA on electroretinogram (ERG) readings (Figure 14). The a-wave reflects the health of the photoreceptors, while the b-wave reflects the health of the inner retinal layers (46). A wide variety of electrodes are available to record voltage responses from the cornea or sclera when exposed to bright light. The ERG of patients with a retinopathy like AMD may display an irregular b-wave with reduced amplitude. This study could examine whether GPR143 signaling influences the b-wave in patients with AMD.

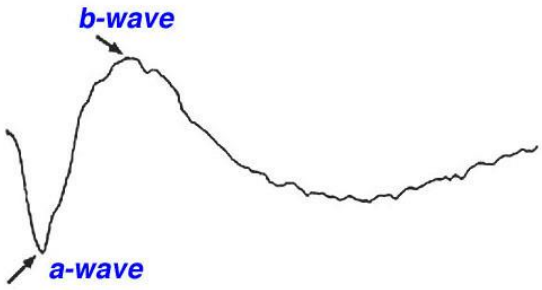

Figure 14. ERG reading, adapted from Creel (2012). Illustrates the expected biphasic waveform of a healthy patient.

7. Conclusion

Although more than 8.7% of the global population has AMD, there is still no cure for the disease. Currently, the most common treatment for AMD is anti-VEGF therapy, which is both

expensive and painful. Based on a retrospective electronic medical record analysis and prospective clinical trial, L-DOPA appears to be a promising therapy that is pain-free, inexpensive, and effective. To better understand the mechanisms by which L-DOPA protects against AMD, this project sought to investigate whether GPR143 signaling alters the rate of POS digestion by the RPE. Our results suggest that L-DOPA does not affect the phagocytosis of POS. However, L-DOPA likely contributes to more efficient endosomal trafficking of the POS to the lysosome, leading to faster clearance and recycling. Further pursuing this avenue of research may aid in attaining a deeper understanding of how L-DOPA positively affects AMD.

References

1. Klein R, Klein BEK. The prevalence of age-related eye diseases and visual impairment in aging: current estimates. Invest Ophthalmol Vis Sci [Internet]. 2013 Dec 13 [cited 2022 Apr 10];54(14). Available from: https://pubmed.ncbi.nlm.nih.gov/24335069/

2. Resnikoff S, Pascolini D, Etya' D, Kocur I, Pararajasegaram R, Pokharel GP, et al. Global data on visual impairment in the year 2002. Bull World Health Organ. 2004;82(11).

3. Jager RD, Mieler WF, Miller JW. Medical progress: Age-related macular degeneration. New England Journal of Medicine. 2008;358(24).

4. Kovach JL, Schwartz SG, Flynn HW, Scott IU. Anti-VEGF Treatment Strategies for Wet AMD. Journal of Ophthalmology. 2012;2012.

5. Martin DF, Ying G shuang, Grunwald JE, Jaffe GJ. Ranibizumab and Bevacizumab for Neovascular Age-Related Macular Degeneration. n engl j med. 2011;20:1897–908.

6. Mitchell P, Korobelnik JF, Lanzetta P, Holz FG, Prünte C, Schmidt-Erfurth U, et al. Ranibizumab (Lucentis) in neovascular age-related macular degeneration: evidence from clinical trials. Available from: http://bjo.bmj.com/

7. Bergen AA, Arya S, Koster C, Pilgrim MG, Wiatrek-Moumoulidis D, van der Spek PJ, et al. On the origin of proteins in human drusen: The meet, greet and stick hypothesis. Progress in Retinal and Eye Research [Internet]. 2019 May 1 [cited 2022 Apr 10];70:55–84. Available from: https://doi.org/10.1016/j.preteyeres.2018.12.003

8. Frank RN, Puklin JE, Stock C, Canter LA, Klein R, Ferris FL, et al. Race, iris color, and age-related macular degeneration. Trans Am Ophthalmol Soc [Internet]. 2000 [cited 2022 Apr 10];98:109. Available from: /pmc/articles/PMC1298217/?report=abstract

9. Chang MA, Bressler SB, Munoz B, West SK. Racial differences and other risk factors for incidence and progression of age-related macular degeneration: Salisbury Eye Evaluation (SEE) Project. Invest Ophthalmol Vis Sci [Internet]. 2008 Jun [cited 2022 Apr 10];49(6):2395–402. Available from: https://pubmed.ncbi.nlm.nih.gov/18263809/

10. Milton RC, Clemons TE, Klien R, Seddon JM, Ferris FL. Risk factors for the incidence of Advanced Age-Related Macular Degeneration in the Age-Related Eye Disease Study (AREDS) AREDS report no. 19. Ophthalmology [Internet]. 2005 [cited 2022 Apr 10];112(4):533-539.e1. Available from: https://pubmed.ncbi.nlm.nih.gov/15808240/

11. Fisher DE, Klein BEK, Wong TY, Rotter JI, Li X, Shrager S, et al. Incidence of Age-Related Macular Degeneration in a Multi-Ethnic United States Population: The Multi-

Ethnic Study of Atherosclerosis. Ophthalmology [Internet]. 2016 Jun 1 [cited 2022 Apr 10];123(6):1297–308. Available from: https://pubmed.ncbi.nlm.nih.gov/26896123/

12. McKay BS, Schwartz SG. Pigmentation and Macular Degeneration: Is There a Role for GPR143? J Ocul Pharmacol Ther [Internet]. 2016 Jan 1 [cited 2022 Apr 10];32(1):3–4. Available from: https://pubmed.ncbi.nlm.nih.gov/26741053/

13. Figueroa AG, McKay BS. A G-Protein Coupled Receptor and Macular Degeneration. Cells [Internet]. 2020 Apr 8 [cited 2022 Apr 10];9(4). Available from: https://pubmed.ncbi.nlm.nih.gov/32276449/

14. Chew EY, Clemons TE, Agrón E, Sperduto RD, Sangiovanni JP, Kurinij N, et al. Long-term effects of vitamins C and E, β-carotene, and zinc on age-related macular degeneration: AREDS report no. 35. Ophthalmology [Internet]. 2013 [cited 2022 Apr 10];120(8). Available from: https://pubmed.ncbi.nlm.nih.gov/23582353/

15. Rofagha S, Bhisitkul RB, Boyer DS, Sadda SR, Zhang K. Seven-Year Outcomes in Ranibizumab-Treated Patients in ANCHOR, MARINA, and HORIZON A Multicenter Cohort Study (SEVEN-UP). Ophthalmology [Internet]. 2013;120:2292–9. Available from: http://dx.doi.org/10.1016/j.ophtha.2013.03.046

16. Lopez VM, Decatur CL, Stamer WD, Lynch RM, McKay BS. L-DOPA is an endogenous ligand for OA1. PLoS Biol [Internet]. 2008 Sep [cited 2022 Apr 10];6(9):1861–9. Available from: https://pubmed.ncbi.nlm.nih.gov/18828673/

17. Mazzoni F, Safa H, Finnemann SC. Understanding photoreceptor outer segment phagocytosis: Use and utility of RPE cells in culture. Exp Eye Res [Internet]. 2014 [cited 2022 Apr 10];0:51. Available from: /pmc/articles/PMC4145030/

18. Schiaffino MV, Baschirotto C, Pellegrini G, Montalti S, Tacchetti C, de Luca M, et al. The ocular albinism type 1 gene product is a membrane glycoprotein localized to melanosomes. Proc Natl Acad Sci U S A [Internet]. 1996 Aug 20 [cited 2022 Apr 10];93(17):9055. Available from: /pmc/articles/PMC38594/?report=abstract

19. Schiaffino MV, Tacchetti C. The ocular albinism type 1 (OA1) protein and the evidence for an intracellular signal transduction system involved in melanosome biogenesis. Pigment Cell Res [Internet]. 2005 Aug [cited 2022 Apr 10];18(4):227–33. Available from: https://pubmed.ncbi.nlm.nih.gov/16029416/

20. Lee H, Scott J, Griffiths H, Self JE, Lotery A. Oral levodopa rescues retinal morphology and visual function in a murine model of human albinism. 2019; Available from: www.ifpcs.orgoratwww.societymelanomaresarch.orghttp://mc.manuscriptcentral.com/pcmr

21. Falk T, Congrove NR, Zhang S, McCourt AD, Sherman SJ, McKay BS. PEDF and VEGF-A output from human retinal pigment epithelial cells grown on novel microcarriers. J Biomed Biotechnol [Internet]. 2012 [cited 2022 Apr 10];2012. Available from: https://pubmed.ncbi.nlm.nih.gov/22547925/

22. Creel DJ, Summers CG, King RA. Visual anomalies associated with albinism. Ophthalmic Paediatr Genet [Internet]. 1990 [cited 2022 Apr 11];11(3):193–200. Available from: https://pubmed.ncbi.nlm.nih.gov/2280977/

23. Brilliant MH, Vaziri K, Connor TB, Schwartz SG, Carroll JJ, McCarty CA, et al. Mining Retrospective Data for Virtual Prospective Drug Repurposing: L-DOPA and Age-related Macular Degeneration. American Journal of Medicine. 2016;129(3).

24. Figueroa AG, Boyd BM, Christensen CA, Javid CG, McKay BS, Fagan TC, et al. Levodopa Positively Affects Neovascular Age-Related Macular Degeneration. American Journal of Medicine. 2021;134(1).

25. Kiel JW. The Ocular Circulation. The Ocular Circulation [Internet]. 2010 [cited 2022 Apr 10]; Available from: https://www.ncbi.nlm.nih.gov/books/NBK53323/

26. Lens A, Nemeth SC, Ledford JK. Ocular anatomy and physiology [Internet]. SLACK Incorporated. 2008. p. 1–4. Available from: https://onesearch.nihlibrary.ors.nih.gov/discovery/fulldisplay?vid=01NIH_INST:NIH&tab=NIHCampus&docid=alma991000528579704686&lang=en&context=L&adaptor=Local%20Search%20Engine&query=sub,exact,%20Retina%20-%20cytology%20,AND&mode=advanced

27. Delamere NA. Ciliary Body and Ciliary Epithelium. Adv Organ Biol [Internet]. 2005 [cited 2022 Apr 10];10:127. Available from: /pmc/articles/PMC3018825/

28. Strenk SA, Strenk LM, Koretz JF. The mechanism of presbyopia. Progress in Retinal and Eye Research. 2005 May 1;24(3):379–93.

29. Boulton M, Dayhaw-Barker P. The role of the retinal pigment epithelium: topographical variation and ageing changes. 2001.

30. Guha S, Liu J, Baltazar G, Laties AM, Mitchell CH. Rescue of compromised lysosomes enhances degradation of photoreceptor outer segments and reduces lipofuscin-like autofluorescence in retinal pigmented epithelial cells. Adv Exp Med Biol [Internet]. 2014 [cited 2022 Apr 10];801:105–11. Available from: https://pubmed.ncbi.nlm.nih.gov/24664687/

31. Nguyen-Legros J, Hicks D. Renewal of photoreceptor outer segments and their phagocytosis by theretinal pigment epithelium. International Review of Cytology. 2000 Jan 1;196:245–313.

32. Balkema G, Bunt-Milam A. Cone outer segment shedding in the goldfish retina characterized with the 3H-fucose technique [Internet]. [cited 2022 Apr 10]. Available from: https://iovs.arvojournals.org/article.aspx?articleid=2159325

33. Figueroa AG, McKay BS. A G-Protein Coupled Receptor and Macular Degeneration. Vol. 9, Cells. 2020.

34. Kevany BM, Palczewski K. Phagocytosis of retinal rod and cone photoreceptors. Vol. 25, Physiology. 2010.

35. Young RW, Bok D. Participation of the retinal pigment epithelium in the rod outer segment renewal process. J Cell Biol. 1969;42(2).

36. Nandrot EF, Anand M, Almeida D, Atabai K, Sheppard D, Finnemann SC. Essential role for MFG-E8 as ligand for αvβ5 integrin in diurnal retinal phagocytosis. Proc Natl Acad Sci U S A [Internet]. 2007 Jul 17 [cited 2022 Apr 10];104(29):12005. Available from: /pmc/articles/PMC1924559/

37. Ryeom SW, Sparrow JR, Silverstein RL. CD36 participates in the phagocytosis of rod outer segments by retinal pigment epithelium. Journal of Cell Science [Internet]. 1996 Feb 1 [cited 2022 Apr 10];109(2):387–95. Available from: https://journals.biologists.com/jcs/article/109/2/387/24728/CD36-participates-in-the-phagocytosis-of-rod-outer

38. Hall MO, Obin MS, Heeb MJ, Burgess BL, Abrams TA. Both protein S and Gas6 stimulate outer segment phagocytosis by cultured rat retinal pigment epithelial cells. Experimental Eye Research [Internet]. 2005 Nov [cited 2022 Apr 10];81(5):581–91. Available from: www.elsevier.com/locate/yexer

39. Regan CM, de Grip WJ, Daemen FJM, Bonting SL. Degradation of rhodopsin by a lysosomal fraction of retinal pigment epithelium: Biochemical aspects of the visual process. XLI. Experimental Eye Research. 1980 Feb 1;30(2):183–91.

40. Parinot C, Rieu Q, Chatagnon J, Finnemann SC, Nandrot EF. Large-Scale Purification of Porcine or Bovine Photoreceptor Outer Segments for Phagocytosis Assays on Retinal Pigment Epithelial Cells. Journal of Visualized Experiments : JoVE [Internet]. 2014 Dec 12 [cited 2022 Apr 10];(94):52100. Available from: /pmc/articles/PMC4396958/

41. Lu SY, Wan HC, Li M, Lin YL. Subcellular localization of Mitf in monocytic cells. Histochemistry and Cell Biology [Internet]. 2010 Jun [cited 2022 Apr 10];133(6):651. Available from: /pmc/articles/PMC2869019/

42. Shen B, Rosenberg B, Orlow SJ. Intracellular Distribution and Late Endosomal Effects of the Ocular Albinism Type 1 Gene Product: Consequences of Disease-Causing Mutations and Implications for Melanosome Biogenesis. Traffic. 2001;2:202–11.

43. Stenmark H, Olkkonen VM. The Rab GTPase family. Genome Biology [Internet]. 2001;2(5). Available from: http://genomebiology.com/2001/2/5/reviews/3007.1http://genomebiology.com/2001/2/5/reviews/3007

44. Mondal S, Hsiao K, Goueli SA. A Homogenous Bioluminescent System for Measuring GTPase, GTPase Activating Protein, and Guanine Nucleotide Exchange Factor Activities.

45. Hayasaka S, Hara S, Mizuno K. Degradation of Rod Outer Segment Proteins by Cathepsin D. The Journal of Biochemistry [Internet]. 1975 Dec 1 [cited 2022 Apr 20];78(6):1365–7. Available from: https://academic.oup.com/jb/article/78/6/1365/830062

46. Creel DJ. The Electroretinogram and Electro-oculogram: Clinical Applications [Internet]. Available from: https://webvision.med.utah.edu/book/electrophysiology/the-electroretinogram-clinical-applications/